Ab initio simulation of first-order amorphous-to-amorphous phase transition of silicon

Murat Durandurdu
Department of Physics and Astronomy, Condensed Matter and Surface Science Program, Ohio University, Athens, Ohio 45701

D. A. Drabold
Trinity College, Cambridge, CB2 1TQ, United Kingdom
and Department of Physics and Astronomy, Ohio University, Athens, Ohio 45701
(Received 5 December 2000; revised manuscript received 28 March 2001; published 1 June 2001)

The pressure-induced phase transition in amorphous silicon (*a*-Si) is studied using *ab initio* constant-pressure molecular-dynamic simulations. Crystalline silicon (*c*-Si) shows a phase transformation from diamond-to-simple hexagonal at 29.5 GPa, whereas *a*-Si presents an irreversible sharp transition to an amorphous metallic phase at 16.25 GPa. The transition pressure of *a*-Si is also calculated from the Gibbs free energy curves and it is found that the transformation takes place at about 9 GPa in good agreement with the experimental result of 10 GPa. We also study the electronic character of the pressure-induced insulator to metal transition.

DOI: 10.1103/PhysRevB.64.014101 PACS number(s): 64.70.Dv, 61.43.Dq, 64.70.Kb

I. INTRODUCTION

Many questions persist about pressure-induced phase transitions in materials. An energetic experimental and theoretical effort has been directed to these questions, and much progress has been made. An exception is the case of pressure-induced phase transition in disordered materials, a case for which there is some experimental information, but very little theory. In the specific context of the classic amorphous semiconductor amorphous silicon (*a*-Si), we use current first-principles techniques to address the following questions. (1) In a system which has native topological disorder, how does the system topology change under pressure? (2) Is the transition first or second order? (3) How does the insulator-metal (electronic) transition proceed in the high-pressure amorphous phase?

For the crystal, the diamond $\rightarrow\beta$-Sn$\rightarrow Imma \rightarrow$simple hexagonal (SH)$\rightarrow$Si(VI)$\rightarrow$HCP transitions have been observed experimentally[1–4] and successfully explained from the first principles calculations.[5,6] Recently, molecular-dynamics (MD) simulations have made it possible to observe directly the dynamical character of the solid-solid pressure-induced phase transition. Focher *et al.*,[9] and Morishita *et al.*,[10] performed a first-principles constant pressure MD for crystalline silicon (*c*-Si) using Parrinello-Rahman (PR) method[11]which enables the simulation cell to change volume and shape and found that the diamond structure of *c*-Si transforms into the SH phase at 30 and 26 GPa, respectively.

There are also some studies on high-pressure phase transformation of the silicon clathrate Si_{136}. Dong *et al.*, have shown recently a transformation from Si_{136} to β-Sn at about 3–4 GPa and diamond to Si_{136} near -4 GPa using a first-principles calculation.[7,8]

Where *a*-Si is concerned, the pressure-induced phase transition is less clearly understood than in *c*-Si. Although thin films of *a*-Si and *a*-Ge exhibit an amorphous to crystalline phase transition at room temperature,[14–17] experiments have shown that a dense amorphous structure can form depending on the temperature.[17]

In this paper, we present an *ab initio* constant pressure MD study of semiconductor to metal transition in *c*-Si and *a*-Si. To our knowledge, this is the first direct MD simulation to study the pressure-induced phase transition in *a*-Si. *c*-Si initially arranged in the diamond structure undergoes a first-order phase transition to the SH structure at 29.5 GPa and *a*-Si presents a discontinuous transition to an amorphous metallic phase at 16.25 GPa. The calculated transformation is in excellent agreement with the experimental observation that the semiconductor-metal transition in the amorphous materials (Si and Ge) arise from structural modification between amorphous phases.[14,15] The energy-volume calculation predicts that the transition pressure of *a*-Si is about 9 GPa which is consistent with the experimental value of 10 GPa.[14,15] In contrast to *c*-Si, the *a*-Si network suffers the gradual change of the coordination number because of its nonuniform environment. The optical gap of *c*-Si decreases gradually under pressure, whereas that of *a*-Si first increases smoothly, then reaches a maximum and decreases with pressure. The modification of the bond lengths, of the bond angles and of the coordination number under pressure is responsible for the behavior of the optical gap in *a*-Si. It is also found that the highly localized conduction tail states of *a*-Si become delocalized with increase of pressure.

II. METHODOLOGY

The simulations reported here are carried out in a 216-atom model of *c*-Si and *a*-Si. The *a*-Si model is due to Djordjevic *et al.* and is in uniform agreement with structural, vibrational, and optical measurements.[18] At zero pressure, the amorphous cell is equilibrated and relaxed with a local orbital first principles quantum MD method, FIREBALL96,[19] designed for application to large complex system. The method employs density functional theory within the local density approximation and hard norm-conserving pseudopotentials.

 ©2001 The American Physical Society

The method is implemented entirely real space. The short-range nonorthogonal single-ζ ($1s+3p$ per site) local orbital basis of compact slightly excited *fireball* orbitals of Sankey and Niklewski offers an accurate description of the chemistry with a significant computational advantage,[20] ideal for the complex system. This method has been successfully applied in *c*-Si including high pressure phases,[20] expanded volume phases of silicon (''zeolites without oxygen''),[21] silicon clusters,[22,23] *a*-Si,[24,25] and in a wide range of other amorphous systems, *a*-GaN,[26] *a*-C,[27] and $GeSe_2$.[28,29] Slow dynamical quenching starting at 800 K under constant pressure is performed to fully relax the systems to zero temperature. The number of steps required to optimize the structures depends on the pressure, and near the transition required about 10 000 time steps. The number of steps was selected to ensure that the system was completely relaxed (according to the criterion that the maximum force was smaller in magnitude than 0.01 eV/Å). Naturally, more steps were required near the transition when dramatic structural rearrangements were observed. All the calculations used soley the Γ point to sample the Brillouin zone, which is reasonable for a cubic cell with 216 atoms. A fictitious cell mass of 6×10^3 amu was found to be suitable for these simulations. With a candidate high pressure phase in hand, the transition pressure can be calculated from the well-known thermodynamic theorem that the phase transformation occurs when the Gibbs free energy

$$G=E_{\mathrm{tot}}+PV-TS \tag{1}$$

becomes equal between the two phases.

In order to characterize the localization of electronic states through the transition, we define the Mulliken charge[31] $Q(n,E)$ for atom n associated with the eigenvalue E. Here,

$$Q_2(E)=N\sum_{n=1}^{N} Q(n,E)^2, \tag{2}$$

where N is the number of atoms in a supercell. For a uniformly extended state, $Q_2(E)$ is 1, while it is N for a state perfectly localized on a single atom.

As with all calculations of the type we report here, there are limitations associated with the size of the cell, the duration of the MD run, and approximations in the Hamiltonian employed. Probably the most serious limitation is the accessible time of the MD run (and implicitly an imperfect sampling of possible conformations). It is never possible to completely rule out ''missing a phase'' though we think that it is very unlikely to be relevant here because of the consistency of our work with experiments and comparisons of our high pressure simulations on *c*-Si, and other published work on *c*-Si. The cell size for this paper is large by the standards of *ab initio* MD, and adequate to induce only small biasing from size artifacts. The Hamiltonian we use has been extensively tested on a wide variety of Si systems and consistently does very well, despite a minimal basis.

TABLE I. Structural properties of *c*-Si under pressure: average bond length (ABL), average bond angle (ABA), bond angle distribution width (BAD), and average coordination number (ACN).

Pressure (GPa)	0	10	15	17	29.5
ABL (Å)	2.377	2.319	2.289	2.278	2.479
ABA	109.48°	109.47°	109.4°	109.4°	100.6°
BAD	0.018	0.033	2.24	2.72	34.49
ACN	4.0	4.0	4.0	4.0	8.0

III. RESULTS AND DISCUSSIONS

A. Structural properties of *c*-Si under pressure

As a preliminary, we repeated the high pressure computations of others for *c*-Si. We find that the diamond structure remains essentially intact until about 17 GPa with a small bond angle distortion. After the system is fully relaxed we study structural relaxation as a function of pressure. At 29.5 GPa a dramatic structural change is observed: the diamond structure transforms to SH in agreement with the previous constant pressure MD calculations.[9,10] However, the SH structure contains defects. The structural properties of *c*-Si under pressure is summarized in Table I. The average bond length increases to 2.479 Å which is close to the experimental result of $a=2.463$ Å for a SH structure at 36 GPa (Ref. 32) but, less than $a=2.667$ Å and $c=2.547$ Å for a perfect SH at equilibrium volume.[33] It is found that the normalized volume to measured zero-pressure volume ($V^{\mathrm{SH}}/V^{\mathrm{diamond}}$)is 0.62 which is slightly lower than the previous first principle calculations 0.672–0.69.[6]

B. Structural properties of *a*-Si under pressure

For a more reliable estimate of the transition pressure, we first plot the pressure-volume curve in Fig. 1. The volume changes smoothly up to 16.25 GPa. At this pressure, an abrupt decline of the volume is seen indicating a first-order pressure-induced phase transition. The behavior of the normalized volume is in excellent agreement with the experiment, but the metastable transition pressure is higher than the experimental value of 10 GPa.[14,15] In order to obtain an equilibrium critical transition pressure we calculate the Gibbs free energy of amorphous phase and the high pressure phase at zero temperature. The Gibbs free energy curves (Fig. 1) cross at about 9 GPa, indicating a transition, which is in good agreement with the experimental result of 10 GPa.[14,15] The large value of the metastable (Parrinello-Rahman) transition pressure implies an intrinsic activation barrier for transforming one solid phase into another .[9,13,12] The thermodynamic theorem gives the density of the high pressure phase at transition as 3.2 g/cm^3 which is less than 3.42 g/cm^3 predicted from the MD. This implies that the cell is superpressured because of the activation energy, well above the transition pressure where two structure coexist, in analogy to isobaric superheating in MD simulations.[12] The pressure-volume curves from slow pressure release at 17 GPa is given in Fig. 1. The path is not reversed because of the strain-induced disappearance of the local minima of the potential energy

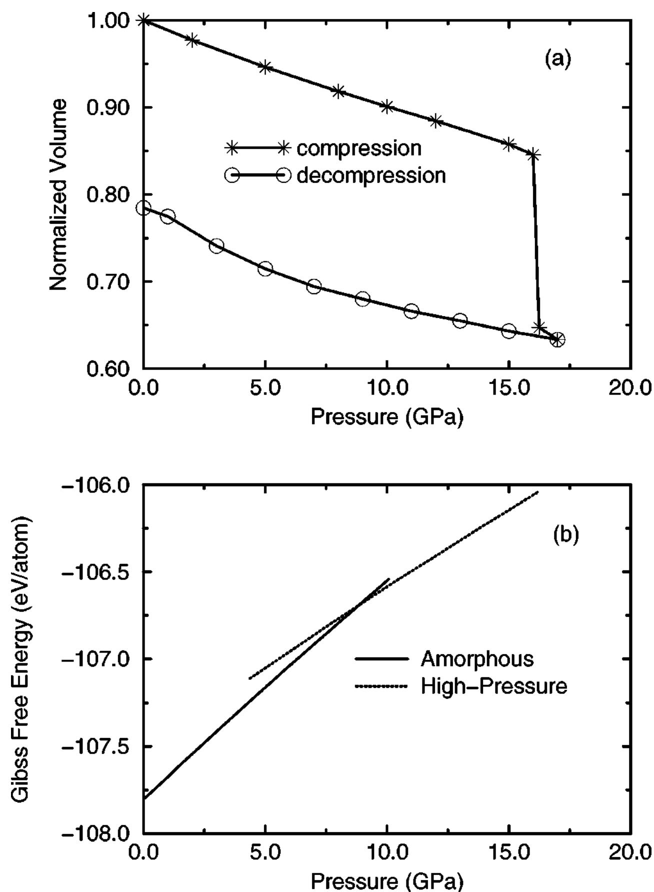

FIG. 1. (a) The normalized volume of *a*-Si to the zero-pressure measured volume. At 16.25 GPa, the volume drops suddenly, indicating pressure-induced phase transition. (b) Gibbs free energy of amorphous and high pressure phase cross near 9 GPa implying a transition.

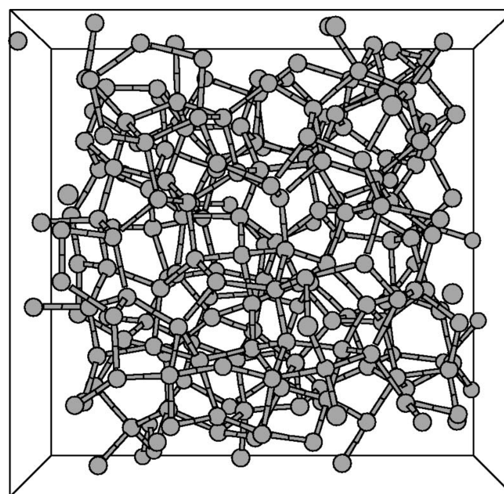

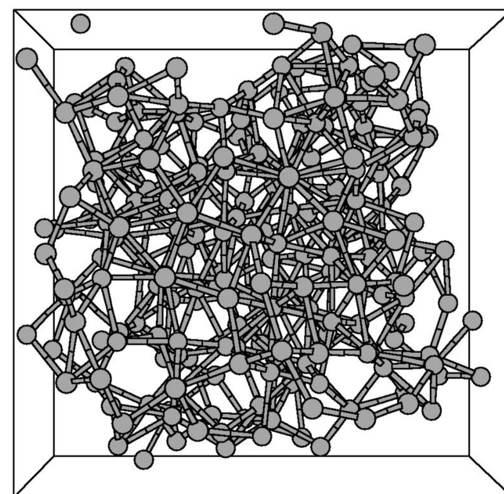

FIG. 2. (a) *a*-Si model at zero pressure. (b) The disordered high pressure phase at 16.25 GPa.

surface.[35] Similar irreversible transitions have been observed in *a*-Ge,[16] SiO_2,[35,36] GeO_2,[37] and H_2O (Ref. 38) which shows a first-order phase change from the low-density amorphous (LDA) to a high-density amorphous (HDA). The density difference between HDA and LDA phase of H_2O is almost 25%. Here, the phase from the slow pressure release is 27% denser than the amorphous phase. It also is found that the fast pressure release from 16.25 to 0 GPa and 17 to 0 GPa gives 21.6% and 22.7% more dense structure. Nevertheless the decompression started from different final pressures gives very similar structure albeit with small difference in density and coordination. In Fig. 2, we illustrate the zero-pressure amorphous phase and metallic amorphous phase.

The pressure dependence of the total energy per atom of *a*-Si is given in Fig. 3. The energy increases nonlinearly with pressure. The energy of *a*-Si branch and the energy of the high pressure phase branch are separated by a gap which gives the energy barrier of transformation for the system. The energy gap between two branches is found to be about 0.25 eV.

The pair distribution function is given in Fig. 4. The peak positions shift to shorter distances, indicating tighter packing of the network, with pressure up to 16.25 GPa. The intensity of the peaks changes slightly until the transition pressure at which a huge coordination change is observed. At the transition pressure the intensity of the first peak drops suddenly with broad distribution and its position shifts into a larger distance, reflecting a much higher ($\approx 8-9$ fold) coordination. The intensity of the second peak exhibits a sharp decrease and shifts to a shorter distance. The result is consistent with x-ray diffraction of SiO_2 glass at high pressure, which reveals an increase of the first neighbor and a decrease of the second neighbor separation.[34] It is of interest to compare the pair distribution function of the zero-pressure phase from the slow pressure release with that of *a*-Si. The nearest-neighbor peak is narrowed, with slight decrease of the intensity. Dramatic changes are seen in the second and third shell: both show broad distribution with increase in the second shell intensity and decrease in the third shell intensity.

The bond angle distribution function of *a*-Si is given in Fig. 4. The perfectly coordinated model at 0 GPa shows a smooth distribution with a single peak centered at the tetrahedral angle. The function develops several peaks under pressure as a result of the increase of the coordination. At

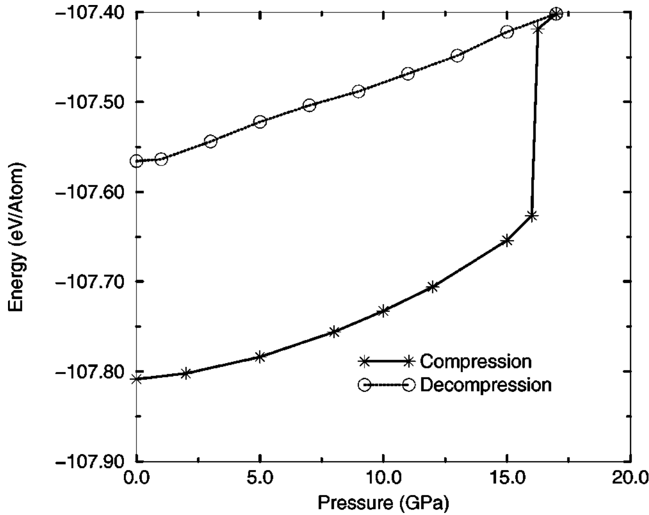

FIG. 3. The pressure dependence of the total energy per atom for *a*-Si and the high pressure phase.

16.25 GPa, the function is rather broad with main peaks around 60°, 90°, and 150°. Car-Parrinello (CP) (Ref. 39) and Fabricius *et al.*, in their respective *ab initio* MD (Ref. 40) simulation report that the bond angle distribution function of liquid-Silicon (*l*-Si) has a prominent peak around 60° followed by a broad distribution with a single maximum containing a bump at near 150°. Although the general shape of both bond angle distribution functions is similar, there are two main differences between them: the bond angle distribution function of the our model induces a small peak near 150° rather than a shoulder and the intensity at 60° is rather larger because of the higher coordination. On decompression we notice that the intensity at 60° and 90° present drastic change: the intensity at 60° decreases while that at 90° increases.

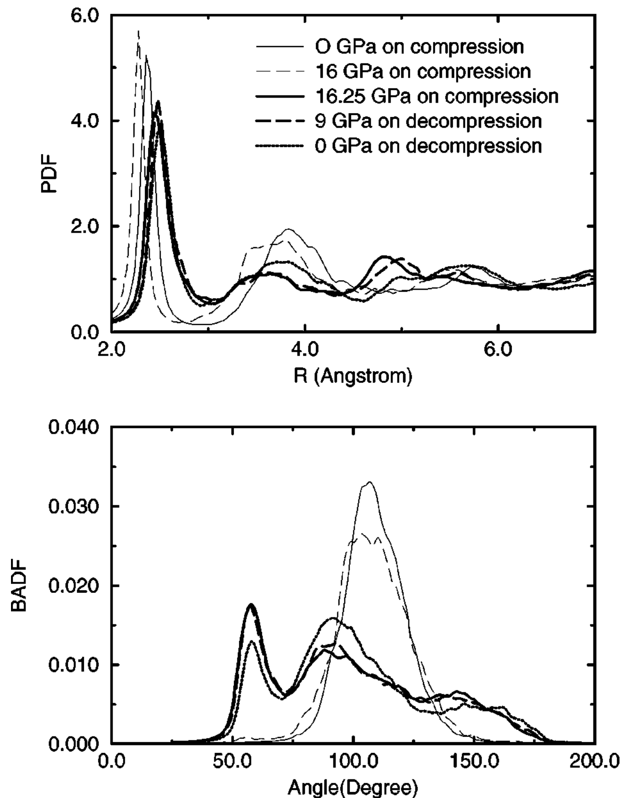

FIG. 4. (a) The behavior of the pair distribution function (PDF) of and (b) the bond angle distribution function (BADF) of *a*-Si on compression and slow decompression.

TABLE II. Structural properties of *a*-Si under pressure. Same nomenclature as Table I.

Pressure (GPa)	0	8	16	16.25	17
ABL (Å)	2.386	2.328	2.290	2.540	2.560
ABA	109.17°	108.93°	108.3°	98.23°	97.88°
BAD	11.1	12.1	14.2	32.9	33.0
ACN	4.0	4.0	4.1	8.6	9.2

Table II presents the structural properties of *a*-Si model under pressure. The initial compression causes the narrowing of tetrahedral angles, shortened bond lengths and slightly increased coordination. At 16.25 GPa, the average bond angle drops to 98.23° which is intermediate between the tetrahedral and octohedral values of 109.5° and 90°, respectively. The average coordination from the pair distribution function (coordination radius $R_c = 3.02$ Å) for the high pressure phase of *a*-Si is 8.6, which is larger than the experimental value of 6.4 (Ref. 41) and CP simulation result of 6.5 (Ref. 39) for *l*-Si. This is unsurprising since the density of the high pressure phase ($3.42 g/cm^3$) is larger than that of *l*-Si (2.59 g/cm^3).[39] The structural properties of the zero-pressure phases on decompression are given in Table III. The densified phases at zero-pressure present a small fluctuation in the average bond angle and average bond length, but $\sim 27-30\%$ decrease in the average coordination number.

The behavior of *c*-Si and *a*-Si network under pressure is rather different. In contrast to *c*-Si, *a*-Si network presents some local modification, gradual increase of the coordination. In spite of the small local modification, the transformation occurs globally in *a*-Si as it is observed in *c*-Si. In *a*-Si, we find that the increase of the coordination occurs first in the vicinity of defects with large bond angle deviations. The highly stressed part of the model has a tendency to transform to a more closed packed geometry under pressure since the angle distortions provide paths for the increases of the coordination.

The energies of the optimized structures at several volumes fit the Birch-Murnaghan equation of states.[30] The obtained bulk modulus of *c*-Si, 97.56 GPa, is consistent with

TABLE III. Structural properties of the obtained zero-pressure phases on decompression. Same nomenclature as Table I.

Pressure (GPa)	17 to 0	16.25 to 0	17 to 0 slowly
ABL (Å)	2.55	2.54	2.55
ABA	100.9°	101.6°	100.9°
BAD	30.9	30.4	31.2
ACN	5.98	5.72	6.25

the experimental value of 98 GPa. We find that the bulk modulus of *a*-Si, 82.5 GPa, is less than that of *c*-Si as expected. The calculated bulk modulus of the high pressure phase of *a*-Si, 77.15 GPa, is smaller than that of *a*-Si. The softening of the bulk modulus in the high pressure phase of *a*-Si can not be explained as a free-volume effect and it is due to the high coordination, which leads to additional restrictions to the bulk relaxation in the distorted networks.[42]

C. The pressure dependence of band gap energy

Atomistic simulation also allows us to directly study the electronic nature of the pressure-induced insulator-metal transition. It is found that both conduction and valence tail states shift into higher energies at low pressure range in *a*-Si. The shift of the conduction tail states is larger than the valence tail states, implying an increase of the optical gap. Under higher pressure, the conduction tail states move to lower energies while the valence tail states continue to shift to higher energies, yielding a decrease of the band gap energy. In *c*-Si network, the bonding and anti-bonding energy separation decreases with increase of overlap from pressure. Simultaneously the conduction and valence band both broaden. The change to metallic structure takes place in a gradual way.

In tetrahedral materials, the effect of the pressure on optical absorption edges is small and pressure derivatives of the energy are nearly zero.[16,43,44,46] These characteristics are ascribed to rigid three dimensional bonding structure. In amorphous tetrahedral materials including *a*-Si, the optical gap increases and the refractive index decreases with pressure (0–1 GPa).[43] The pressure coefficient of the fundamental absorption in *a*-Si is positive, +0.25 meV/kbar,[43] whereas it is negative in*c*-Si, -1.5 meV/kbar,[43] and in *a*-Si:H, −1 meV/kbar.[46,45] Figure 5 shows the pressure dependence of the optical gap in *c*-Si and *a*-Si. The gap of *c*-Si decreases smoothly with pressure. We find the pressure derivative of the gap for *c*-Si is -1.73 meV/kbar in the pressure range 0–17 GPa. This value is the same in the sign, but slightly different in magnitude what is reported in Ref. 43. The gap behavior of the optical gap width in *a*-Si under pressure is nonlinear. For low pressures, it increases gradually and reaches a maximum at 5 GPa. Under further compression, the gap decreases because of structural change.

D. Localized states in *a*-Si and response to pressure

The measure of the localization of the states is shown in Fig. 6. Each spike on the figure represents an energy eigenvalue. The larger $Q_2(E)$ for a state, the more spatially localized it is. As expected, the states near midgap are quite localized at zero pressure. The localization of the conduction tail states shows a decrease with increase of the pressure up to 16.25 GPa, implying the pressure-induced delocalization of the states. The pressure dependence of average inverse participation ratio is given in Fig. 5. At 16.25 GPa, all states are completely extended. The tiny gap in Fig. 6 (at 16.25 GPa) is a finite size and single-ζ (minimal basis) artifact: the material is certainly conducting.

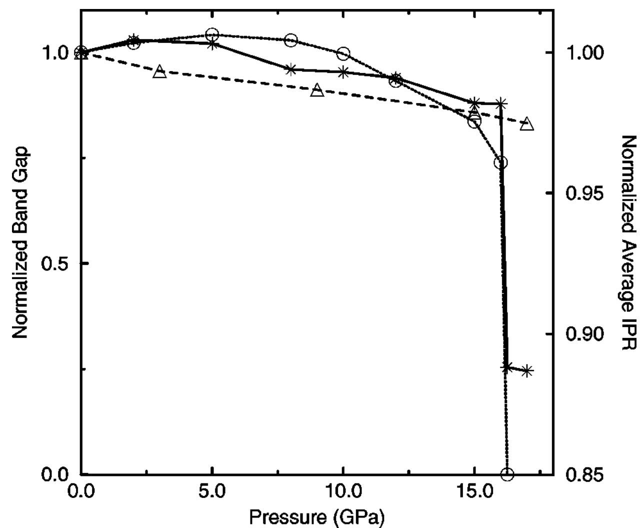

FIG. 5. Pressure dependence of the normalized optical gap to zero-pressure optical gap for *c*-Si (dashed line with triangle) for *a*-Si (dotted line with circle) and the normalized average inverse participation ratio (solid line with star).

E. Vibrational density of states

It is valuable to predict the phonon modes for *a*-Si, the high pressure phase, and *c*-Si. The physical origin of the

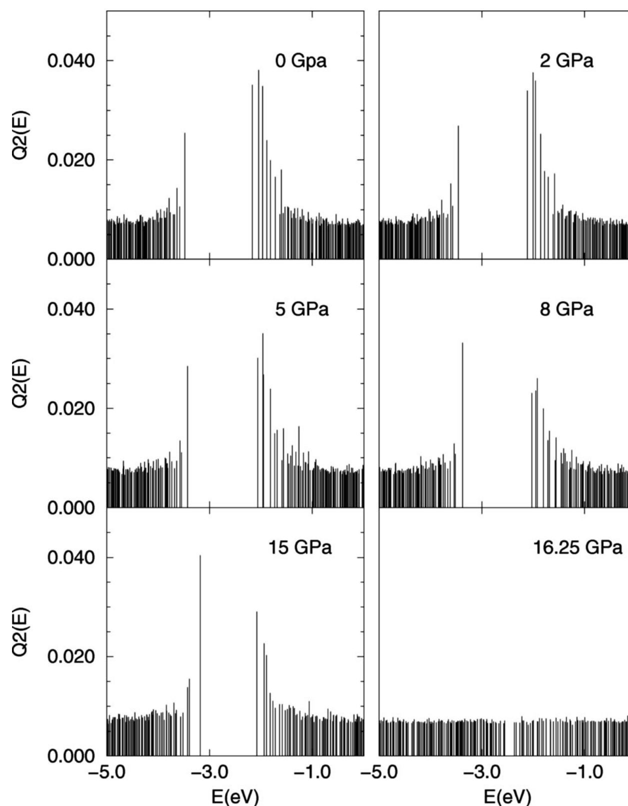

FIG. 6. Electronic eigenstates in the band gap region. The position of vertical bars represents the eigenvalues of the electronic eigenstates and height of the bars is the spatial localization $Q_2(E)$. The Fermi level lies in the middle of the band gap. Note the abrupt delocalization of tail states at 16.25 GPa.

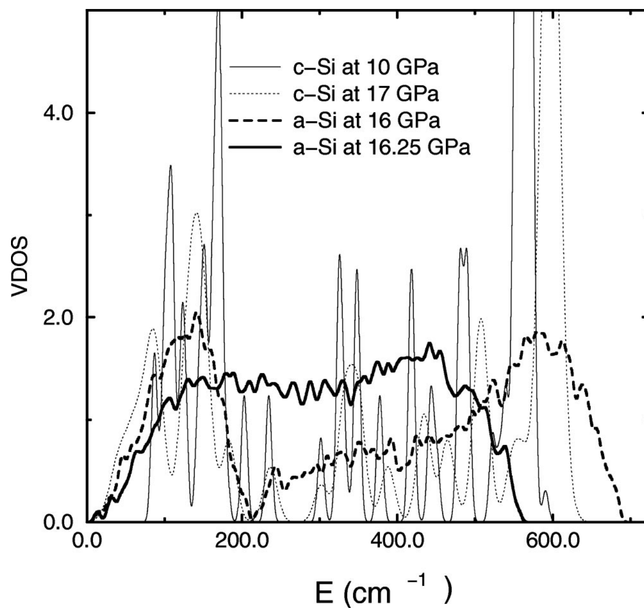

FIG. 7. Vibrational DOS of *a*-Si at 16 GPa and the high pressure phase at 16.25 GPa and *c*-Si at 10 and 17 GPa.

phase transition can be understood by examining the pressure sensitive soft phonon modes. The vibrational density of states (VDOS) is given in Fig. 7. With increase of pressure in *c*-Si, the acoustic modes are softened, while optical modes shift to higher energy. The results are consistent with Raman scattering.[47] We notice large decrease of the energy of the optical band and a small increase of the energy of the acoustical band in *a*-Si. This can be in principle be compared indirectly to Raman measurement.

IV. CONCLUSIONS

We have studied the pressure-induced phase transition in *c*-Si and *a*-Si with *ab initio* constant pressure MD technique. *a*-Si undergoes a first-order phase transition into an amorphous metallic phase while *c*-Si transforms into the SH structure at 29.5 GPa. The obtained amorphous to amorphous phase transition is irreversible. The behavior of *a*-Si network under pressure is rather different from that of *c*-Si because of its environment. The defects in *a*-Si behave as nucleation centers for pressure-induced change. It is found that the localized conduction tail states become extended with pressure.

ACKNOWLEDGMENTS

We thank Professor Jianjun Dong and Professor N. Mousseau for advice and many helpful discussions and Dr. A. A. Demkov and Professor O. F. Sankey for the PR method implementation in the FIREBALL96. This work was supported by the National Science Foundation under Grant No. DMR-00-81006 and DMR-0074624.

[1] M. C. Gupta and A. L. Ruoff, J. Appl. Phys. **51**, 1072 (1980).
[2] H. Olijnyk, S. K. Sikka, and W. B. Holzapfel, Phys. Lett. A **103**, 137 (1987).
[3] J. Z. Hu, L. D. Merkle, C. S. Menoni, and I. L. Spain, Phys. Rev. B **34**, 4679 (1986); J. Z. Hu and I. L. Spain, Solid State Commun. **51**, 263 (1984).
[4] M. I. McMahon and R. J. Nelmes, Phys. Rev. B **47**, 8337 (1993); M. I. McMahon, R. J. Nelmes, N. G. Wright, and D. R. Allan, *ibid.* **50**, 739 (1994).
[5] M. T. Yin and M. L. Cohen, Phys. Rev. Lett. **45**, 1004 (1980).
[6] K. J. Chang and M. L. Cohen, Phys. Rev. B **31**, 7819 (1985).
[7] G. Ramachadran, P. F. McMillan, S. K. Deb, M. Somayazulu, J. Gryko, Jianjun Dong, and O. T. Sankey, J. Phys.: Condens. Matter **12**, 4013 (2000).
[8] Jianjun Dong, O. F. Sankey, and G. Kern, Phys. Rev. B **60**, 950 (1999).
[9] P. Focher, G. L. Chiarotti, M. Bernasconi, E. Tosatti, and M. Parrinello, Europhys. Lett. **26**, 345 (1994).
[10] T. Morishita and S. Nosé, Prog. Theor. Phys. Suppl. **138**, 251 (2000).
[11] M. Parrinello and A. Rahman, Phys. Rev. Lett. **45**, 1196 (1980); S. Nose and M. L. Klein, Mol. Phys. **50**, 1055 (1983).
[12] I. H. Lee, J. W. Jeong, and K. J. Chang, Phys. Rev. B **55**, 5689 (1997).
[13] K. Mizushima, S. Yip, and E. Kaxiras, Phys. Rev. B **50**, 14 952 (1994).
[14] O. Shimomura, S. Minomura, N. Sakai, K. Asaumi, K. Tamura, J. Fukushima, and H. Endo, Philos. Mag. **29**, 547 (1974).
[15] S. Minomura, *High pressure and Low-Temperature Physics* (Plenum, New York, 1978), p. 483.
[16] K. Tanaka, Phys. Rev. B **43**, 4302 (1991).
[17] K. Tanaka, J Non-Cryst. Solids **150**, 44 (1992).
[18] B. R. Djordjevic, M. F. Thorpe, and F. Wooten, Phys. Rev. B **52**, 5685 (1995).
[19] A. A. Demkov, J. Ortega, O. F. Sankey, and M. P. Grumbach, Phys. Rev. B **52**, 1618 (1995).
[20] O. F. Sankey and D. J. Niklewski, Phys. Rev. B **40**, 3979 (1989).
[21] A. A. Demkov, W. Windl, and O. F. Sankey, Phys. Rev. B **53**, 11 288 (1996).
[22] J. Song, S. E. Ulloa, and D. A. Drabold, Phys. Rev. B **53**, 8042 (1996).
[23] M. Yu, S. E. Ulloa, and D. A. Drabold, Phys. Rev. B **61**, 2626 (2000).
[24] P. A. Fedders, D. A. Drabold, and S. Nakhmanson, Phys. Rev. B **58**, 15 624 (1998).
[25] M. Durandurdu, D. A. Drabold, and N. Mousseau, Phys. Rev. B **62**, 15 307 (2000).
[26] P. Stumm and D. A. Drabold, Phys. Rev. Lett. **79**, 677 (1997).
[27] D. A. Drabold, P. A. Fedders, and P. Stumm, Phys. Rev. B **49**, 16 415 (1994).
[28] M. Cobb and D. A. Drabold, Phys. Rev. B **56**, 3054 (1997).
[29] X. Zhang and D. A. Drabold, Phys. Rev. B **62**, 15 695 (2000).
[30] F. Birch, J. Geophys. Res. **57**, 227 (1952).
[31] A. Szabo and N. S. Ostlund, *Modern Quantum Chemistry* (Dover, New York, 1996).

[32] S. J. Duclos, Y. K. Vohra, and A. L. Ruoff, Phys. Rev. B **41**, 12 021 (1990).
[33] F. Zandiehnadem and W. Y. Ching, Phys. Rev. B **41**, 12 162 (1990).
[34] C. Meade, R. J. Hemley, and H. K. Mao, Phys. Rev. Lett. **69**, 1387 (1992).
[35] D. J. Lacks, Phys. Rev. Lett. **84**, 4629 (2000); **80**, 5385 (1998).
[36] P. McMillan, B. Piriou, and R. Couty, J. Chem. Phys. **81**, 4234 (1984).
[37] O. B. Tsiok, V. V. Brazhkin, A. G. Lyapin, and L. G. Khvostantsev, Phys. Rev. Lett. **80**, 999 (1998).
[38] O. Mishima, L. D. Calvert, and W. Whalley, Nature (London) **314**, 76 (1985).
[39] I. Stich, R. Car, and M. Parrinello, Phys. Rev. Lett. **63**, 2240 (1989); Phys. Rev. B **44**, 4262 (1991).
[40] G. Fabricius, E. Artacho, D. Sanchez-Portal, P. Ordejon, D. A. Drabold, and J. M. Soler, Phys. Rev. B **60**, R16 283 (1999).
[41] Y. Waseda and K. Suzuki, Z. Phys. B **20**, 339 (1975).
[42] V. V. Brazhkin, A. G. Lyapin, V. A. Goncharova, O. V. Stal'gorova, and S. V. Popova, Phys. Rev. B **56**, 990 (1997).
[43] G. A. Connel and W. Paul, J. Non-Cryst. Solids **8-10**, 215 (1972).
[44] T. Tanaka, J. Non-Cryst. Solids **90**, 363 (1987).
[45] S. Minomura, J. Phys. (Paris), Colloq. **42**, C4-181 (1981); in *Semiconductors and Semimetals*, edited by J. I. Pankove (Academic, Orlando, 1984), Vol. 21A, p. 273.
[46] T. Tanaka and S. Nitta, Phys. Rev. B **39**, 3258 (1989).
[47] B. Weinstein and G. J. Piermarini, Phys. Rev. B **12**, 1172 (1975).